

# Novel Ecological Tiles Made with Granite Fine Quarry Waste and Oil Palm Fiber Ash

**Danupon Tonnayopas, Kalayanee Kooptarnond and Mahamasuhaimee Masae**

Department of Mining and Materials Engineering, Faculty of Engineering,

Prince of Songkla University, Hat-Yai, 90112 Thailand.

E-mail: danupon.t@psu.ac.th

## Abstract

Floor tile body recipes were prepared using granite fine quarry waste (GFQW) and oil palm fiber ash (OPFA) as raw materials with clearly defined physical and chemical properties at single sieve residues and different fast fired temperatures under industrial conditions. The most suitable formulations with the corresponding optimum moisture contents were determined and further fired at different peak temperatures under laboratory conditions in order to establish their vitrification ranges and optimum firing temperatures. The tested peak firing temperatures were varied at 20°C intervals from 1140 to 1180°C for floor tile bodies. The physical and thermal properties of the fired bodies such as colour, water absorption, linear firing shrinkage, and bulk density were measured. Furthermore, consideration was given to the phase and microstructural evolution of the developed tile bodies. X-ray fluorescence, and X-ray diffraction (XRD) in combination with thermogravimetry were used to analyse the phases formed before and after firing. The experimental results showed that it was possible to obtain a floor tile body with the properties in accordance with TIS 37-2529.

**Keywords:** oil palm fiber ash, granite fine quarry waste, temperature, floor tiles, micro-structure

## 1. Introduction

According to the analysis of the domestic and overseas research and achievements, some wastes are similar in composition to the natural raw materials used in the ceramic tiles [1-4]. These materials are not only compatible but also beneficial in the fabrication of them. Therefore, upgrading industrial wastes to alternative ceramic raw materials becomes interesting, both technically and economically, for a wide range of applications [5]. Waste materials for the ceramic industry have been classified into three categories

[6]: fuel ash waste with high contents of organic or carbon-rich substances, with high calorific added-value; fluxing wastes (improve sinterability of ceramic body, or glassy phase former); and plasticity controlling waste which affect green body preparation, (likely shrinkage controller), both drying and firing.

The southern Thailand region is an area that has a large quantity of granite quarries. A growing amount of granite fine quarry waste (GFQW) reaches up to 15wt.% of the aggregate production.

Another type of waste, which derives from the large palm oil factories in

southern Thailand, approximately 5% of oil palm fiber ash (OPFA) is carried out of the boiler (around 800°C) by flue gases in order to generate steam for thermoelectric energy in a factory operation. It needs to be disposed of in a landfill outside the factory premises so that it causes the least disturbances to the main factory operation. The best solution of the disposal problem of GFQW and OPFA is to decrease the quantity for disposal with utilization of both wastes in industry. Hence, more productive use of them would have environmental benefits such as reducing air, water and land pollution. Many previous works have cited GFQW and other ash waste in the production of ceramics [7-10] and tiles [11-17].

The objective of this work is to further investigate the use of GFQW as alternative ceramic raw materials in the ceramic tile production and find out the optimum OPFA incorporation of the tile, without degrading their properties based upon the Thai Industrial Standard (TIS).

## 2. Experimental

### Raw Material

The GFQW sample was taken from raw material stockpiled in the production area, which were generated in a crushing process of granite quarry (Wang Pai), located about 15 km from Chana district, Songkhla and OPFA incorporated in the tile body was provided from the waste of burning of oil palm fiber fuel in the boiler of the Nam Hong Palm Oil Industry Company, situated in Khao Phanom district, Krabi province. These raw materials were dried in an air oven at 110°C for 8 h, the GFQW was ground in a ball mill for 3 h and then each of them was sieved through mesh 200. Afterwards, both raw materials were submitted to the following characterization techniques, including chemical composition obtained by X-ray fluorescence (XRF, Philips

Model PW2400), and mineral composition identified by X-ray diffraction (XRD, Philips X'Pert MPD). The particle size distribution was measured by a laser diffraction analyzer (Beckman Coulter LS 230). The differential thermal analysis (DTA) of the OPFA sample was simultaneously conducted in a DTA model PerkinElmer, DTA7 instrument operating under a flow of nitrogen (20 ml/min) and heating rate of 10°C/min until the maximum temperature range, from 30 to 1300°C. Its thermal behavior was also measured on a thermogravimetric analyzer (TG) PerkinElmer, TGA7 at a heating rate of 10°C/min in nitrogen atmosphere, over the temperature range from 50 to 1200°C. GFQW body mixtures containing 0, 10, 20, and 30 wt.% of OPFA were homogenized for 15 min in a dry plastic mixer (Table 1). Moisture was then adjusted, according to the standard compaction test, which is known as optimum moisture content (OMC) [18]. All specimens were cured at room temperature for 24 h and then prepared mixtures were axially pressed into test squares (115 mm × 115 mm × 10 mm in the size of green tile specimens) under pressure of 100 bar (about 10 MPa), and kept in an oven at 105±5°C for 8 h. Subsequently, they were sintered in air for 8 h at 1140°C, 1160°C and 1180°C in an electric furnace under a heating rate of 2°C/min until 500°C, soaked 0.5 hr, and continued with heating rate of 5°C/min until reaching the designed maximum temperature, followed by 0.5 h soaking. The tile specimens were cooled down to room temperature in the furnace. Unfired samples were characterized by the measurement of working moisture [19], drying shrinkage [20], and modulus of rupture [21].

**Table 1:** GFQW tiles mixtures and optimum moisture content recipes

Mixture Items	Raw materials (wt.%)		OMC %
	GFQW	OPFA	
GFQW or OPFA0	100	0	9.00
OPFA10	90	10	11.00
OPFA20	80	20	11.50
OPFA30	70	30	12.70

The following properties were measured on the sixty fired specimens: water absorption, bulk density, linear shrinkage, weight loss, electrical resistance, rebound hardness, Vickers indentation, and modulus of rupture. The water absorption capacity was determined according to TIS procedures [22-23]. The bulk density was measured by dividing the fired mass by the average external volume. The linear shrinkage was obtained by the length of the samples before and after the firing stage using a Vernier caliper OKURA (precision 0.05 mm) [24]. Open porosity and pore size distribution was calculated from water absorption and specific gravity. Furthermore, the electrical resistance was determined by a MegaOhmmeter (C.A 6525). Vickers indentation was used to characterize the hardness ( $H_v$ ) using a digital micro hardness tester (Highwood Brand model HWDM-3). The fired specimens were submitted to appropriate ten constant loads of the 300 g [25] with dwell time of 15 s each one according to ASTM C1327 procedure [26].

Determination of the flexure strength (FS) was carried out by a Universal Testing Machine (HOUNSFIELD H 100KS) using a three point loading device with a constant cross-head speed of 1.8 mm/min. The strength was calculated from the breaking load using the formula:

$$S = 2PL/3bd^2 \quad (1)$$

where  $S$  = flexural strength ( $\text{kgf/cm}^2$ ),  $P$  = load (kg),  $L$  = span (cm),  $b$  = breadth (cm) and  $d$  = thickness (cm).

Moreover, stress intensity factor or fracture toughness ( $K_{IC}$ ) was calculated from the following equation given by ASTM E 399 [27]:

$$d \geq 2.5 \left( \frac{K_{IC}}{\sigma_{YS}} \right)^2 \quad (2)$$

where  $d$  = the specimen thickness;  $\sigma_{YS}$  = the yield strength.

In addition, the major crystalline phases of the selected fire specimens were also identified by XRD. The microstructure characterization of the raw materials and the fracture surfaces of the previous tested specimens was observed by scanning electron microscopy (SEM) using a model JSM-5200, (JEOL).

### 3. Result and Discussion

#### 3.1 Characterization of raw materials

The particle size distribution of OPFA and GFQW are illustrated in Figure 1. The uniformity is rather similar and the main feature of significance is the generally larger particle sizes in the OPFA (between 1 and 16  $\mu\text{m}$ , with average particle size of 9  $\mu\text{m}$ , whereas in the GFQW of 1-36  $\mu\text{m}$ , the average is 23  $\mu\text{m}$ ). It should be kept in mind that the difference in particle size distribution and the non-plastic characteristics of both wastes, particularly for high OPFA contents, might introduce some difficulties in the shaping process.

The mineral composition of GFQW is composed basically of quartz (31.85%), albite (48.83%), microcline (17.54%), and muscovite (1.79%). The OPFA presents a typical composition and is constituted mainly by  $\text{SiO}_2$ ,  $\text{Al}_2\text{O}_3$ ,  $\text{CaO}$ , and  $\text{K}_2\text{O}$ , with small amounts of  $\text{Fe}_2\text{O}_3$  (Table 2). The loss on ignition

(LOI) is higher (3.33%) as the OPFA is associated with volatile components, organic matter and decomposition of carbonates (CaO). The high alkaline earth and alkaline oxide content (CaO and  $K_2O$ ), indicates the flux potential of the OPFA. The significant amount of  $Fe_2O_3$  in both raw materials (2.13 and 3.11%) is responsible for the reddish color of the fired specimens.

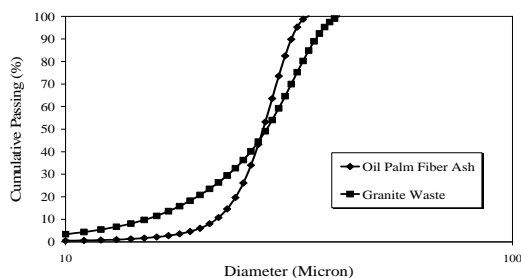


**Figure 1:** Particle size distribution of raw materials

**Table 2:** Main chemical composition of raw materials (wt.%)

Waste Type	GFQW	OPFFA
$SiO_2$	67.91	57.45
$Al_2O_3$	15.07	1.53
$Fe_2O_3$	2.13	3.11
CaO	1.10	12.22
$K_2O$	6.95	12.00
$Na_2O$	5.28	-
LOI	0.77	3.33

However, the DTA thermogram result of OPFA displayed two endothermic events (Figure 2). The first endothermic peak at 989.9°C is suggestive of a polymorphous transformation of carbonate and the last endothermic effect near 1122.7°C was caused by melting ( $T_m$ ), indicating the presence of quartz and feldspars (orthoclase and plagioclase). It can be due to a structural reorganization, cristobalite nucleation. The second effects can be a crystallization process.

Furthermore, for the thermogravimetry (TG) and DTA curves for residue in air atmosphere, the TG curve presents six decomposition stages. The water loss occurred (<1%) in the first stage ( $T_i$  100°C), and in the last five stage (208°C, 399°C, 580°C, 712°C and 973°C) the weight loss was 0.59, 0.63, 0.97, 1.42 and 4.76%, respectively, which can be attributed to the decomposition of carbonates. The TG plot shows a composition of up to 91% which indicates the presence of silicates (quartz, plagioclase, orthoclase and mica). The results obtained from TG and DTA are supported by XRD and XRF studies.

The SEM micrograph of GFQW particles shows irregular forms and sharp smooth surfaces as well as some other show angular corners (Figure 3a). On the contrary, OPFA particles exhibit spherical form, round surfaces and some have pores and subangular corners (Figure 3b).

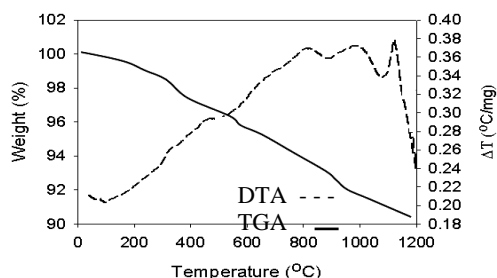


**Figure 2:** Thermal analysis on OPFA

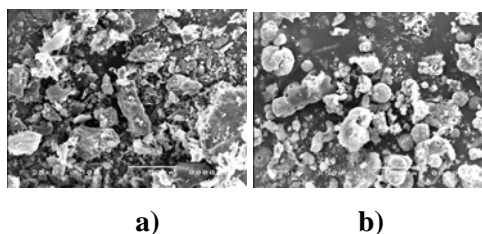


**Figure 3:** SEM photomicrograph of a) GFQW and b) OPFA

### 3.2 Mineralogical identification of tiles

XRD phase analysis was carried out on the OPFA20 tile fired at 1140, 1160 and 1180°C. The material shows the presence of two major crystalline phases, namely, quartz and cristobalite in all of the different fired tile bodies, and microcline residue only at 1140°C. It can be observed that the presence of the peak intensity of cristobalite increased significantly corresponding to the sintered temperature (Figure 4). A possible explanation is the richness in SiO<sub>2</sub> and rather low amounts of the other compositions. The peaks are attributed to the forming of SiO<sub>2</sub> phases.

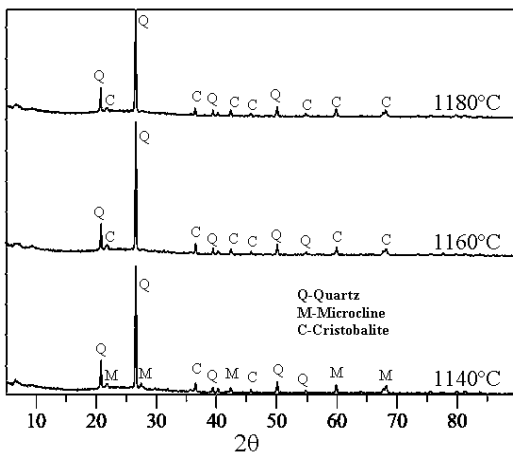


**Figure 4:** X-ray diffraction patterns of OPFA20 tile and sintered at different temperatures.

### 3.3 Physical properties of tiles

The water absorption of GFQW tile ranged from 0.25 of GFQW tile (1180°C) to 0.58 of OPFA30 tile (1140°C). It can be observed that the increase in the OPFA replacement gives rise to an increase in the water absorption, and also depends on the firing temperature (Figure 5a). The water absorption values decrease significantly at 1180°C. This behavior is related to the lower viscosity of the liquid phases produced and the consequently improvement in the densi-

fication process produced at these temperatures. According to TIS-37, the maximum allowed value of water absorption is 3% for commercial use of the floor tile. In particular, GFQW material appears very compact, having a low residual porosity. The temperature effects on the linear shrinkage (Figure 5b), is similar to the weight loss (Figure 5c). It can be seen that the specimens fired at 1140°C to 1180°C displayed similar behaviors, where a dramatically increase of variation in the 0% to 10% OPFA content is noticeable. Nevertheless, less linear shrinkage is a factor that may contribute to reduce the risk of appearance of cracks and dimensional defects in tiles. On the other hand, an excessive amount of OPFA or GFQW can promote cracks due to low particle bonding and, consequently, reduce the mechanical strength.

Variation of bulk density ranged from 1700 kg/m<sup>3</sup> (OPFA30) up to a maximum of 1870 kg/m<sup>3</sup> (GFQW). The increase in the amount of OPFA addition causes a reduction in the tile density (Figure 5d). The main reason for such a result is the burning of OPFA addition as an organic material, which can easily burn out during the sintering period. These bulk density values are, in general, lower than commercial tile and they are a consequence of the particle sintering and microstructure. The total porosity values of tile specimens are in the range of 11.93% (GFQW at 1180°C) to 15.83% (OPFA30 at 1140°C).

The electrical resistance ranged from 1.93 MΩ/mm (GFQW at 1180°C) to 7.61 MΩ/mm (OPFA30 at 1140°C). It can be observed that the increase in OPFA increases the electrical resistance (Figure 5f). Therefore, the increase in water absorption, total porosity, linear shrinkage, weight loss and electrical resistance, as well as the decrease in bulk density with OPFA addition, are a consequence of the

higher changes involved, changing the

texture of recrystallised minerals.

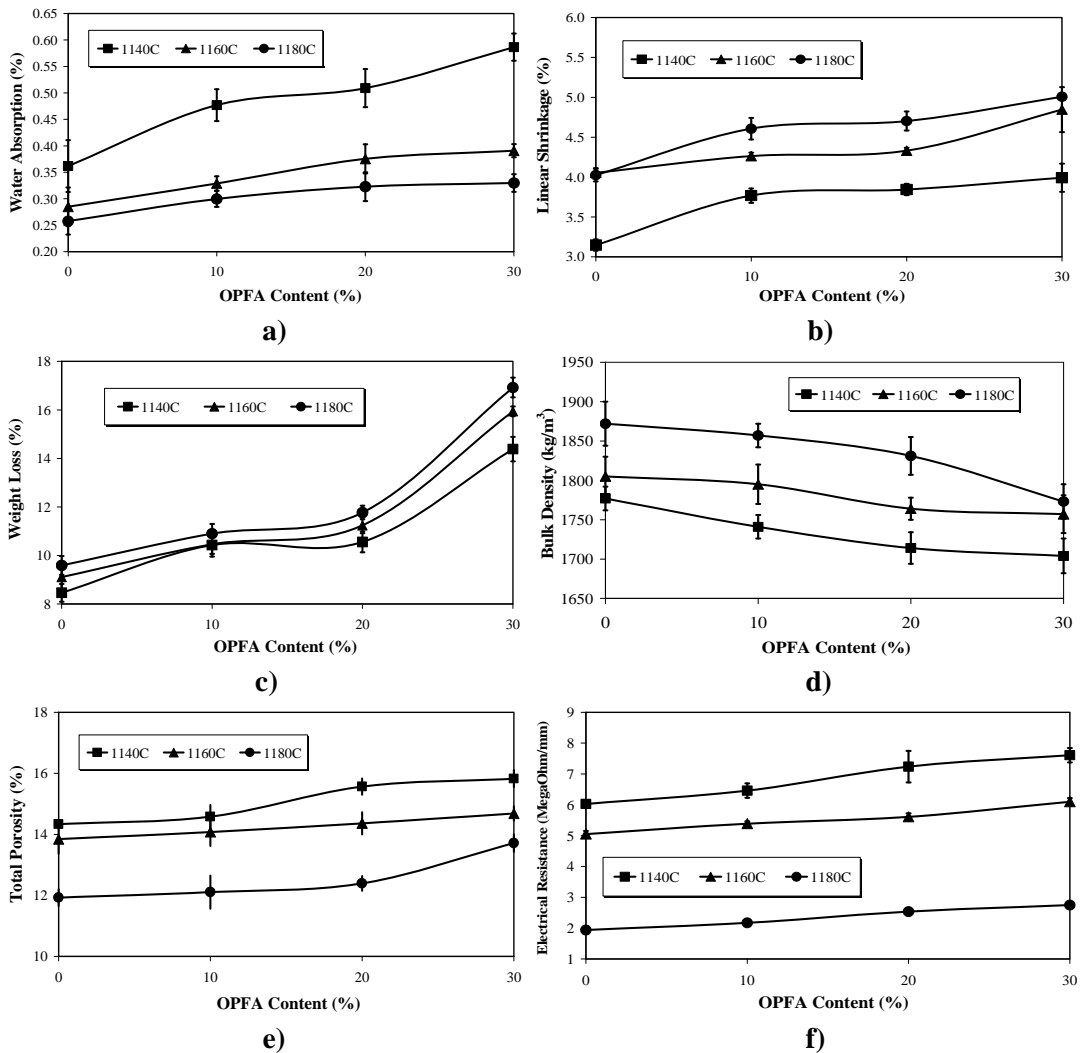


**Figure 5:** Effect of temperature and OPFA content on a) water absorption, b) linear firing shrinkage, c) weight loss, d) bulk density, e) total porosity, and f) electrical resistance of GFQW tiles

### 3.4 Mechanical properties of tiles

Vickers hardness ranged from 5.06 GPa of OPFA30 tile to 5.44 GPa of GFQW tile. Rebound hardness is between 230 HV (OPFA30 at 1140°C) to 468 HV (GFQW at 1180°C). Both Vickers hardness (Figure 6a) and rebound hardness (Figure 6b) decreased followed by an

increase with the growth of the OPFA content, despite the firing temperature.

Furthermore, the modulus of rupture (MOR) values vary from 19.61 to 39.26 MPa, where the highest values are displayed for the specimens fired at 1180°C with OPFA20 tile (Figure 6c). All fired temperature curves show some increase and decrease in MOR with the

increase of OPFA content. Nevertheless, at temperatures above 1140°C, there is transformation from quartz to cristobalite, which has a considerably high strength due to mineral recrystallization (Figure 3), and probably the effect of OPFA content becomes secondary. According to Thai standard (TIS 36, TIS 37), it can be observed that, after firing at 1180°C, all tiles can be used as wall ( $\geq 20$  MPa) and floor ( $\geq 25$  MPa) tiles. Otherwise, based on firing at 1160°C, only GFQW, OPFA10 and OPFA20 tiles can be graded as wall tile.

Considering, the OPFA30 tiles, they can be used to produce ceramics with water absorption lower than 3%. At 1140°C, tiles do not have sufficiently high strength values to satisfy the requirements for ceramic tiles. The most interesting results, in the case of  $K_{IC}$ , have been obtained for the OPFA20 materials (at 1180°C), with values in the range of 1.80-2.44 MPa.m<sup>1/2</sup>. Fracture toughness values (Figure 6d) are calculated in a range from 0.94 MPa.m<sup>1/2</sup> (GFQW) to 2.44 MPa.m<sup>1/2</sup> (OPFA20). It looks too high for production of tiles (2.0 MPa.m<sup>1/2</sup>) in spite of no glaze application.

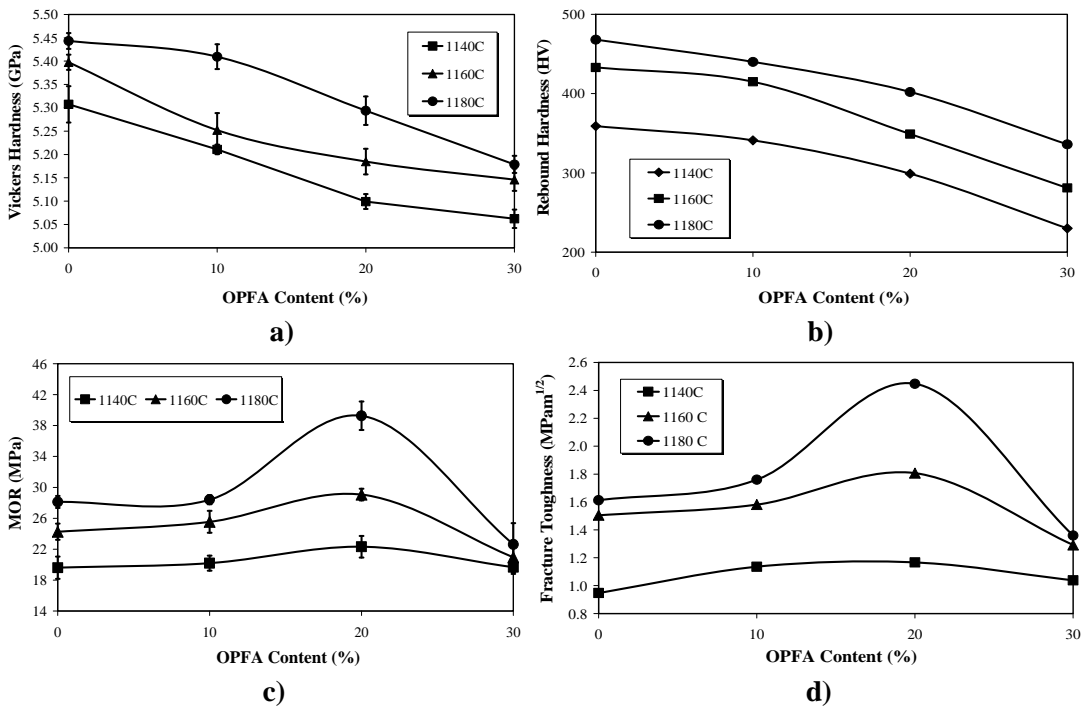


**Figure 6:** Variation of GFQW tiles with firing temperature and OPFA replacement of a) Vickers hardness, b) rebound hardness, c) modulus of rupture and d) fracture toughness

### 3.5 Microstructure of tiles

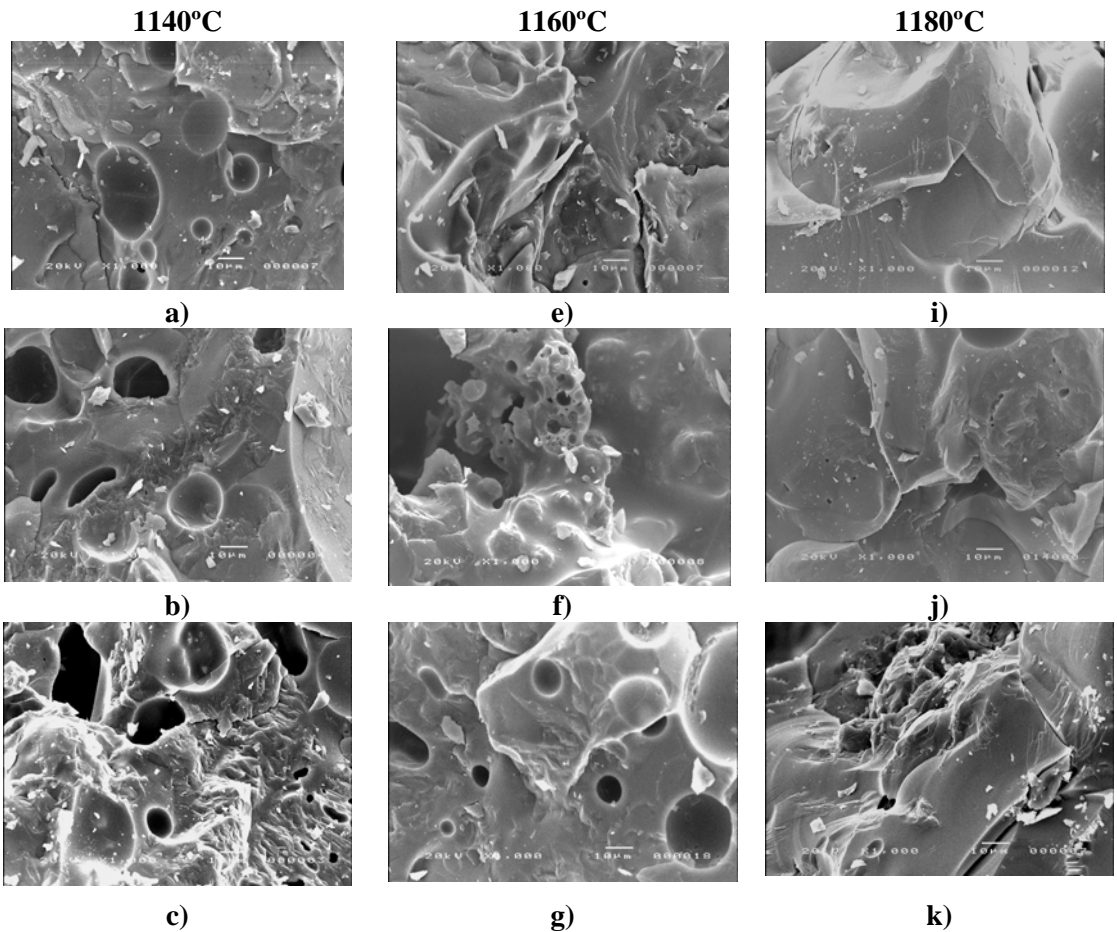
Microstructural observation (Figure 7) on the fracture surface of OPFA20 specimens sintered at 1140°C, 1160°C and 1180°C by SEM revealed the evolution of the sintering process with the rise in the

sintering temperature. The effect is intensified in view of the mass flux from the glass grain to the ceramic matrix, under the exerted capillary forces. Pore formation has been possibly assisted by the formation of gas-bubbles.

For firing at 1140°C, the texture displays a rough microstructure, with insignificant bonding between particles and a lot of interconnecting pores (Figure 7a), an indication that the sintering process has barely started, and of CO<sub>2</sub> gas release during evolution of ceramic texture (Figs. 7b, 7c, 7d). This behaviour is attributed to the unavailability of the crystalline particles to undergo viscous flow [28].

Besides firing at 1160°C, more particles are bonded (grain growth) and the presence of a liquid phase transition at the firing temperature is obvious (round smooth surfaces are characteristic of the presence of liquid during the sintering

process) (Figure 7e). This is a clear sign that the sintering process is underway (Figs. 7f, 7g, 7h). Unlike firing at 1180°C, there are signs of transgranular fracture (strong interface, glassy bonds between grains) and well defined grain boundaries, and many isolated rounded pores can be clearly observed (Figure 7i). The tile texture reached the final sintering stage at this temperature. At 1180°C the specimens present a structure with few pores and signs of vitrification (Figs. 7j, 7k and 7l). As vitrification proceeds, the amount of glassy phase increases and the concentration of dissolved gases in the glassy phase decreases.



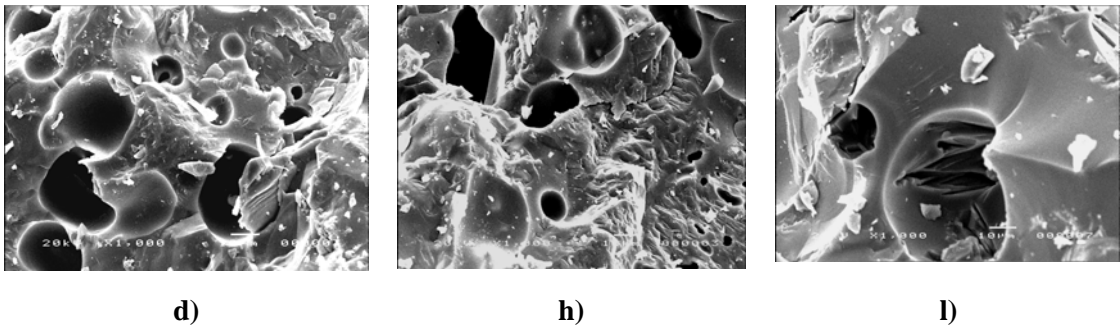


**Figure 7:** Backscattered electron image of the fracture surfaces of OPFA-GFQW tiles fired at 1140°C of OPFA a) 0%, b) 10%, c) 20%, d) 30%; at 1160°C of OPFA e) 0% f) 10%, g) 20%, h) 30% and at 1180°C of OPFA i) 0%, j) 10%, k) 20%, l) 30%

#### 4. Conclusion

The present experimental investigation result in this work, provided the optimal proportion of the GFQW materials in the batch (OPFA20) and firing temperature of 1180°C. The reduction in the vitrification temperature of the mix would also contribute significantly to the economical production of tiles.

The new unglazed GFQW tiles fulfill the requirements of the TIS-36 and -37 standards, (floor and wall tiles) and exhibit superior properties comparing to the commercial ceramic tiles, with regards to water absorption and MOR. There are no major defects of the characteristics of the final product. The GFQW substitutes for some of the expensive minerals used in commercial tile compositions and lowers the product cost. Further, this GFQW is in powder form, thus requiring less grinding time, resulting in energy saving, and more importantly, waste reduction.

#### 5. Acknowledgement

The authors thank the Faculty of Engineering, Prince of Songkla University for financial support of this study. Thanks to The Recycling Materials Research Group (RMRG) Year 3, Department of Mining and Materials Engineering for pro-

viding facilities and laboratory equipment. Special thanks go to Wang Pai quarry and Nam Hong Palm Oil Industry Co., for providing GFQW and OPFA samples, respectively.

#### 6. References

- [1] Fregni, A. and Busani, G., Eco-efficiency of Fabric Filters in the Italian Ceramic Tile Industry, *J. Cleaner Prod.*, Vol. 15, Issue 1, pp. 86-93, 2007.
- [2] Olgun, A., Erdogan, Y., Ayhan, Y. and Zeybek, B., Development of Ceramic Tiles from Coal Fly Ash and Tincal Ore Waste, *Cer. Int.*, Vol. 31, Issue. 1, pp. 153-158, 2005.
- [3] Baruzzo, D., Minichelli, D., Bruckner, S., Fedrizzi, L., Bachiorrini, A. and Maschio, S., Possible Production of Ceramic Tiles from Marine Dredging Spoils Alone and Mixed with Other Waste Materials, *J. Hazard. Mat. B*, Vol. 134, Issue. 1-3, pp. 202-210, 2006
- [4] Sikalidis, C. and Zaspalis, V., Utilization of Mn-Fe Solid Wastes from Electrolytic MnO<sub>2</sub> Production in the Manufacture of Ceramic Building Products, *Constr. and Build. Mat.*, Vol. 21, Issue. 5, pp. 1061-1068, 2007.

- [5] Prasad, C.S., Maiti, K.N. and Venugopal, R., Effect of Substitution of Quartz by Rice Husk Ash and Silica Fume on the Properties of White-ware Composition, *Cer. Int.*, Vol. 29, Issue 8, pp. 907-914, 2003.
- [6] Dondi, M., Marsigli, M. and Fabbri, B., Recycling of Industrial and Urban Waste in Brick Production-A Review, *Tile Brick Int.*, Vol. 13, pp. 218-225, 1997.
- [7] Vieira, C.M.F., Soares, T.M., Sanchez, R. and Monteiro, S.N. Incorporation of Granite Waste in Red Ceramics, *Mat. Sci. and Eng. A*, Vol. 373, Issue. 1-2, pp. 115-121, 2004.
- [8] Segadaes, A.M., Carvalho, M.A. and Acchar, W., Using Marble and Granite Rejects to Enhance the Processing of Clay Products, *Appl. Clay Sci.*, Vol. 30, Issue 1, pp. 42-52, 2005.
- [9] Acchar, W., Viera, F.A. and Hotza, D., Effect of Marble and Granite Sludge in Clay Materials, *Mat. Sci. and Eng. A*, Vol. 419, Issue. 1-2, pp. 306-309, 2006.
- [10] Hernandez-Crespo, M.S. and Rincon, J.Ma., New Porcelainized Stoneware Materials Obtained by Recycling of MSW Incinerator Fly Ashes and Granite Sawing Residues, *Cer. Int.*, Vol. 27, Issue. 6, pp. 713-720, 2001.
- [11] Menezes, R.R., Ferreira, H.S., Neves, G.A., Lira, H.L. and Ferreira, H.C., Use of Granite Sawing Wastes in the Production of Ceramic Bricks and Tiles, *J. Eur. Cer. Soc.*, Vol. 25, Issue 7, pp. 1149-1158, 2005.
- [12] Torres, P., Manjate, R.S., Quaresma, S., Fernandes, H.R. and Ferreira, J.M.F., Development of Ceramic Floor **Tile** Compositions Based on Quartzite and **Granite Sludges**, *J. Eur. Cer. Soc.*, Vol. 27, Issue 16, pp. 4649-4655, 2007.
- [13] Torres, P., Fernandes, H.R., Agathopoulos, S., Tulyaganov, D.U. and Ferreira, J.M.F., Incorporation of Granite Cutting Sludge in Industrial Porcelain Tiles Formulation, *J. Eur. Cer. Soc.*, Vol. 24, Issues 10-11, pp. 3177-3185, 2004.
- [14] Pinatti, D.G., Conte, R.A., Borlini, M.C., Santos, B.C., Oliveira, I., Vieira, C.M.F. and Monteiro, S.N., Incorporation of the Ash from Cellulignin into Vitrified Ceramic Tiles, *J. Eur. Cer. Soc.*, Vol. 26, Issue 3, pp. 305-310, 2006.
- [15] Zimmer, A. and Bergmann, C.P., Fly Ash of Mineral Coal as Ceramic Tiles Raw Material, *Waste Man.*, Vol. 27, Issue. 1, pp. 59-68, 2007.
- [16] Youssef, N.F., Osman, T.A., El-Shimy, E., Utilization of Granite-Basalt Fine Quarry Waste in a Ceramic Floor Tile Mixture. *J. Silicate Industries*, Vol. 69, Issues 1-2, pp. 7-13, 2004.
- [17] Monteiro, S.N., Peçanha, L.A. and Vieira, C.M.F., Reformulation of Roofing Tiles Body with Addition of Granite Waste from Sawing Operations, *J. Eur. Cer. Soc.*, Vol. 24, Issue 8, pp. 2349-2356, 2004.
- [18] ASTM D 698-00a, Standard Test Methods for Laboratory Compaction Characteristics of Soil Using Standard Effort (12,400 ft-lbf/ft<sup>3</sup> (600 kN-m/m<sup>3</sup>))
- [19] ASTM C 324-01, Standard Test Method of Free Moisture Content in Ceramic Whiteware Clays.
- [20] ASTM C 326 -82, Standard test Method for Drying and Firing Shrinkages of Ceramic Whiteware Clays, 1997.
- [21] ASTM C674-90, Flexural Properties of Ceramic Whiteware Materials, 1997.
- [22] TIS standard 36-2516, Standard for Wall Tiles. (in Thai)

- [23] TIS standard 37-2529, Standard for Floor Tiles. (in Thai)
- [24] ASTM, C 67, Standard Methods of Sampling and Testing Brick and Structural Clay Tile. Brick Manufacturing – Part I, 1986.
- [25] Sidjanin, L., Rajnovic, D., Ranogajec, J. and Molnar, E., Measurement of Vickers Hardness on Ceramic Floor Tiles, J. Eur. Cer. Soc., Vol. 27, Issues 2-3, pp. 1767–1773, 2007.
- [26] ASTM C 1327, Standard Test Method for Vickers Indentation Hardness of Advanced Ceramics, 1999.
- [27] ASTM E 399-90, Standard Test Method for Plane-Strain Fracture Toughness of Metallic Materials, 1997.
- [28] Toledo, R., dos Santos, D.R., Faria, R.T., Carrio, J.G., Auler, L.T., Vargas, H., Gas Release During Clay Firing and Evolution of Ceramic Properties, Appl. Clay Sci., Vol. 27, pp. 151–157, 2004.